Coupling Modes and Stoichiometry of Cl^-/HCO_3^- Exchange by slc26a3 and slc26a6

Nikolay Shcheynikov,[1] Youxue Wang,[1] Meeyoung Park,[1] Shigeru B.H. Ko,[2] Michael Dorwart,[1] Satoru Naruse,[2] Philip J. Thomas,[1] and Shmuel Muallem[1]

[1]Department of Physiology, University of Texas Southwestern Medical Center at Dallas, Dallas, TX 75390
[2]Department of Internal Medicine, Nagoya University, Showa-ku, Nagoya 466-8550, Japan

The SLC26 transporters are a family of mostly luminal Cl^- and HCO_3^- transporters. The transport mechanism and the Cl^-/HCO_3^- stoichiometry are not known for any member of the family. To address these questions, we simultaneously measured the HCO_3^- and Cl^- fluxes and the current or membrane potential of slc26a3 and slc26a6 expressed in *Xenopus laevis* oocytes and the current of the transporters expressed in human embryonic kidney 293 cells. slc26a3 mediates a coupled $2Cl^-/1HCO_3^-$ exchanger. The membrane potential modulated the apparent affinity for extracellular Cl^- of Cl^-/HCO_3^- exchange by slc26a3. Interestingly, the replacement of Cl^- with NO_3^- or SCN^- uncoupled the transport, with large NO_3^- and SCN^- currents and low HCO_3^- transport. An apparent uncoupled current was also developed during the incubation of slc26a3-expressing oocytes in HCO_3^--buffered Cl^--free media. These findings were used to develop a turnover cycle for Cl^- and HCO_3^- transport by slc26a3. Cl^- and HCO_3^- flux measurements revealed that slc26a6 mediates a $1Cl^-/2HCO_3^-$ exchange. Accordingly, holding the membrane potential at 40 and −100 mV accelerated and inhibited, respectively, Cl^--mediated HCO_3^- influx, and holding the membrane potential at −100 mV increased HCO_3^--mediated Cl^- influx. These findings indicate that slc26a6 functions as a coupled $1Cl^-/2HCO_3^-$ exchanger. The significance of isoform-specific Cl^- and HCO_3^- transport stoichiometry by slc26a3 and slc26a6 is discussed in the context of diseases of epithelial Cl^- absorption and HCO_3^- secretion.

The Journal of General Physiology

INTRODUCTION

Anion transport and homeostasis is linked to the regulation of pH_i, both of which are crucial for the proper function of the cells. In epithelia, these mechanisms also mediate transcellular Cl^- and HCO_3^- transport. The SLC26 transporters are members of a relatively new family of anion transporters consisting of 10 known members (Mount and Romero, 2004). Members of the family play important roles in many physiological functions, in particular in epithelia. This is evident from the diseases associated with members of the family. Mutations in this family of proteins can result in dystrophic dysplasia (SLC26A2; Superti-Furga et al., 1996), congenital chloride diarrhea (SLC26A3; Makela et al., 2002), Pendred's syndrome (SLC26A4; Everett et a1., 1997), and hearing loss (SLC26A5; Liu et al., 2003). SLC26A4 also participates in renal HCO_3^- absorption (Royaux et al., 2001) and the control of blood pressure (Verlander et al., 2003), whereas slc26a6 is involved in intestinal HCO_3^- and renal oxalate transport (Wang et al., 2005).

Although the anion selectivity is specific for each member of the family, most can transport Cl^- and HCO_3^- (Mount and Romero, 2004). Initially, the family was identified by searching for $SO_4^=$ transporters and identifying SLC26A1 (Bissig et al., 1994). SLC26A2 was found by positional cloning of the gene associated with dystrophic dysplasia (Hästbacka et al., 1994) and was later shown to function as a $SO_4^=$ transporter. Subsequent studies suggested that many SLC26 transporters function as Cl^-/HCO_3^- exchangers, including slc26a3 (Melvin et al., 1999; Ko et al., 2002), SLC26A4 (Soleimani et al., 2001; Ko et al., 2002), SLC26A6 (Ko et al., 2002; Wang et al., 2002), SLC26A7 (Petrovic et al., 2004), and SLC26A9 (Xu et al., 2005). However, more recent studies showed that SLC26A7 functions as an intracellular pH (pH_i)–regulated Cl^- channel (Kim et al., 2005) and that SLC26A1 and SLC26A2 are specific $SO_4^=$ transporters (Regeer et al., 2003; Forlino et al., 2005).

So far, all of the SLC26 transporters examined except SLC26A7 (Petrovic et al., 2004; but see the expression of SLC26A7 in the luminal membrane of the proximal tubules in Dudas et al., 2006) and SLC26A1 (Nakada et al., 2005) are expressed in the luminal membrane of epithelial cells (Mount and Romero, 2004). Transport of Cl^- and HCO_3^- by the SLC26 transporters raised the

Correspondence to Shmuel Muallem:
shmuel.muallem@utsouthwestern.edu

Abbreviations used in this paper: AE1, anion exchanger 1; DIDS, 4,4′-diisothiocyanostilbene-2,2′-disulfonic acid; GFP, green fluorescent protein; HEK, human embryonic kidney.

possibility that these transporters are the long sought luminal Cl^-/HCO_3^- exchangers that mediate epithelial Cl^- absorption and HCO_3^- secretion, such as in the pancreatic and salivary gland ducts (Cook et al., 1994; Melvin et al., 2005; Steward et al., 2005). Epithelial Cl^- absorption and HCO_3^- secretion is intimately regulated by CFTR (Kunzelmann and Mall, 2002; Irokawa et al., 2004; Melvin et al., 2005; Steward et al., 2005), as evident from the lack of these activities in cystic fibrosis (Wilschanski and Durie, 1998; Sokol, 2001). The importance of the SLC26 transporters in epithelial Cl^- absorption and HCO_3^- secretion is further highlighted by the finding that CFTR potently activates the SLC26 transporters (Ko et al., 2002), and, in turn, the SLC26 transporters are potent activators of CFTR (Ko et al., 2004). This mutual regulation is mediated by interaction of the CFTR R domain and the SLC26 solute transporter anti-σ factor antagonist (STAS) domain and is assisted by the binding of CFTR and the SLC26 transporters to PDZ-containing scaffolding proteins (Ko et al., 2004).

To understand the role of the SLC26 transporters in epithelial Cl^- absorption and HCO_3^- secretion, it is absolutely essential to understand their transport mechanism and their Cl^-/HCO_3^- transport stoichiometry. In an initial study, we reported that slc26a3 and slc26a6 are electrogenic Cl^-/HCO_3^- transporters with isoform-specific stoichiometry (Ko et al., 2002). At the same time, Xie et al. (2002) independently reported that slc26a6 is an electrogenic transporter. However, a recent study that examined the properties of slc26a6 and SLC26A6 concluded that slc26a6 and SLC26A6 are electroneutral Cl^-/HCO_3^- exchangers (Chernova et al., 2005). Although the later study contains some apparent internal inconsistencies (see Discussion), the confusion generated requires clarification. More importantly, many fundamental characteristics of these transporters are unknown. For example, we do not know the exact stoichiometry and mode of transport of any of the SLC26 transporters. It is also unclear whether the transport of Cl^- and HCO_3^- by these transports is obligatorily coupled.

The cardinal importance of the SLC26 transporters in epithelial and other cells' physiology demands clarification, especially the mode of transport and their Cl^-/HCO_3^- transport stoichiometry. The Cl^-/HCO_3^- transport stoichiometry will dictate their precise role in epithelial Cl^- absorption and HCO_3^- secretion (Ko et al., 2004; Steward et al., 2005). In this study, we determined the transport mode and Cl^-/HCO_3^- transport stoichiometry of slc26a3 and slc26a6. To this end, we simultaneously measured intracellular Cl^- (Cl^-_i), pH_i, and membrane potential or current. We report that slc26a3 functions as a coupled $2Cl^-/1HCO_3^-$ exchanger that can also mediate uncoupled NO_3^- and SCN^- transport, whereas slc26a6 functions as an electrogenic coupled $1Cl^-/2HCO_3^-$ exchanger.

MATERIALS AND METHODS

The slc26a3 and slc26a6 clones and their cRNA were the same as those used in previous studies (Ko et al., 2002, 2004). The slc26a3 in the pClneo vector was used for expression in human embryonic kidney (HEK) 293 cells and was shuttled to pXBG-ev1 for the preparation of cRNA. The slc26a6 in the pcDNA3 vector was used for expression in HEK293 cells and for the preparation of cRNA. HEK293 cells were transfected with 1 μg cDNA coding for the transporters and 0.5 μM cDNA coding for green fluorescent protein (GFP). The oocytes were injected with 4 ng cRNA per oocyte in a 50-nl volume. 4,4′-diisothiocyanostilbene-2,2′-disulfonic acid (DIDS) was obtained from Invitrogen. The bath solution for HEK293 cells (solution A) contained 145 mM NaCl, 1 mM $MgCl_2$, 1 mM $CaCl_2$, 10 mM HEPES, pH 7.4 (with NaOH), and 10 mM glucose. Cl^--free solutions were prepared by the replacement of Cl^- with gluconate. Solutions containing NO_3^- or SCN^- were prepared by the replacement of NaCl and KCl with the respective NO_3^- and SCN^- salts. HCO_3^--buffered solutions were prepared by replacing 25 mM Na^+-anion with 25 mM Na^+-HCO_3^- and reducing HEPES to 5 mM. HCO_3^--buffered solutions were gassed with 5% CO_2 and 95% O_2. The osmolarity of all solutions was adjusted to 310 mosmol with the major salt. For experiments with *Xenopus laevis* oocytes, the standard HEPES-buffered medium was ND96 composed of 96 mM NaCl, 2 mM KCl, 1.8 mM $CaCl_2$, 1 mM $MgCl_2$, 2.5 mM pyruvate, and 5 mM HEPES-Na, pH 7.5 (Shcheynikov et al., 2004; Kim et al., 2005). The HCO_3^--buffered solution contained 71.0 mM NaCl, 25.0 mM $NaHCO_3$, 2.0 mM KCl, 1.8 mM $CaCl_2$, 1.0 mM $MgCl_2$, and 5.0 mM HEPES-Na, pH 7.5. The Cl^--free and HCO_3^--buffered solution contained 71.0 mM Na-gluconate, 25.0 mM $NaHCO_3$, 2.0 mM K-gluconate, 1.8 mM Ca^{2+}-cyclamate, 1.0 mM $MgSO_4$, and 5.0 mM HEPES-Na, pH 7.5. Solutions were gassed with 5% CO_2/95% O_2.

Cells

HEK293 cells were cultured in Dulbecco's modified Eagle's medium supplemented with 10% FCS and 1% penicillin and streptomycin. For functional studies, HEK293 cells were cotransfected with the SLC26 transporters and a plasmid coding for GFP. GFP fluorescence was used to identify the transfected cells. LipofectAMINE (Invitrogen) was used for transfections. Oocytes were obtained by partial ovariectomy of anesthetized female *Xenopus*. Follicles were removed and defolliculated as described previously (Shcheynikov et al., 2004; Kim et al., 2005). Healthy oocytes in stages V–VI were injected with 1–10 ng cRNA in a final volume of 50 nl. Injected oocytes were incubated at 18°C in a ND96 solution, and oocytes were used 48–120 h after injection.

Current Measurement in HEK293 Cells

The whole cell configuration of the patch clamp technique was used to measure the Cl^-, NO_3^-, and oxalate currents in HEK293 cells as described previously (Ko et al., 2004). The pipette solution contained 140 mM $NMDG^+$-Cl^- or $NMDG^+$-NO_3^-, 1 mM $MgCl_2$, 2 mM EGTA, 5 mM ATP, and 10 mM HEPES, pH 7.3 (with Tris). The bath solution was Na^+-free solution A. The current was recorded using a patch clamp amplifier (Axopatch 200A; Axon Instruments, Inc.) and digitized at 2 kHz. The membrane conductance was probed by stepping the membrane potential from a holding potential of 0 mV to membrane potentials between −80 and 60 mV at 10-mV steps for 200 ms, with 500-ms intervals between steps. Pipettes had resistance between 5–7 MΩ when filled with pipette solution, and seal resistance was always >8 GΩ. Current recording and analysis were performed with pClamp 6.0.3 software (Axon Instruments, Inc.). Results were analyzed, and figures were plotted with Origin 7.5 software (OriginLab).

Measurement of Current and Membrane Potential in Oocytes

Electrophysiological recordings were performed at room temperature with two-electrode voltage clamp or current clamp methods using an Oocyte Clamp System (OC-725C; Warner Instrument Corp.) as described previously (Ko et al., 2002; Shcheynikov et al., 2004). The microelectrodes were filled with 3 M KCl and had a resistance of 0.5–2 MΩ. Current and voltage were digitized via an A/D converter (Digidata 1322A; Axon Instruments, Inc.) and analyzed using the Clampex 8.1 system (Axon Instruments, Inc.).

Measurement of pH_i and Cl_i in Oocytes

For pH_i and Cl^-_i measurements, electrodes were prepared from single-barreled borosilicate glass tubes (outer diameter = 1.2 mm; inner diameter = 0.69 mm; Warner Instrument Corp.) as described previously (Shcheynikov et al., 2004). In brief, the electrodes were vapor silanized with bis(dimethylamino)dimethyl silane, and the tips of the pH electrodes were filled with 0.5 μl of a H^+ exchanger resin (hydrogen ionophore I, cocktail B; Fluka Chemical Corp.). The electrodes were backfilled with a ND-96 solution and calibrated in standard fresh solutions of pH 6, 7, and 8 before and after each experiment. The electrodes were fitted with a holder with an Ag–AgCl wire attached to a high-impedance probe of a two-channel electrometer (FD-223; World Precision Instruments). A second channel was used for the measurement of membrane potential by standard reference microelectrodes. The bath was grounded via a 3-M KCl agar bridge connected to an Ag–AgCl wire. The signal from the voltage electrode was subtracted from the voltage of the pH electrode using Origin 5.0 or 7.5 software (OriginLab). Initial rates of pH_i change were determined from the slope of the line obtained by fitting pH as a function of time to a linear regression line. The slope of the pH electrodes was between 56 and 57 mV (pH unit)$^{-1}$. To calculate HCO_3^- fluxes, the total buffer capacity (β_T) of the oocytes was determined from the change of pH_i on exposure to CO_2/HCO_3^- (Roos and Boron, 1981) and averaged 39.6 ± 1.3 mM/pH unit (n = 52) at the pH_i attained by incubation in HCO_3^--buffered media of 6.81 ± 0.02.

Cl^-_i was measured with a Cl^--sensitive liquid ion exchanger (477913; Corning) as described previously (Ianowski et al., 2002), with minor modifications. The tips of vapor-silanized electrodes were filled with the Cl^--selective liquid ion exchanger and backfilled with 3 M KCl. The electrodes were calibrated in solutions prepared to contain 1, 3, 10, 30, and 100 mM Cl^- by mixing solutions containing 100 mM KCl and 100 mM K-gluconate. A similar procedure was used to prepare the NO_3^- calibration solutions. Fresh calibration solutions were prepared each experimental day. The slope of the Cl^- microelectrode was ~56 mV per 10-fold change in Cl^- concentration. An example of the calibration curve for Cl^- and NO_3^- is shown in Fig. 1 A. Intracellular Cl^- activity was calculated according to the equation $Cl^-_i = Cl^-_{cal} \times 10^{(\Delta V/S)}$ (Ianowski et al., 2002), where Cl^-_i is intracellular Cl^- activity, Cl^-_{cal} is the Cl^- activity in of the calibration solutions (the Cl^- activity coefficient for the 10- and 100-mM KCl solutions used are 0.77 and 0.901, respectively; Hamer and Wu, 1972), ΔV is the difference in voltage between the Cl^- electrode and reference electrode, and S is the slope measured in response to a 10-fold change in Cl^- activity. Cl^- calibrations were performed in HEPES- and HCO_3^--buffered solutions.

For simultaneous measurement of pH_i and Cl^-_i in oocytes, a three-electrode method was used. In this case, two ion-sensitive electrodes were connected with the FD-223 electrometer, and one reference microelectrode was used to record membrane potential with the OC-725C amplifier (Warner Instrument Corp.).

Statistical Analysis

Results in all experiments are given as the mean ± SEM of the indicated number of experiments.

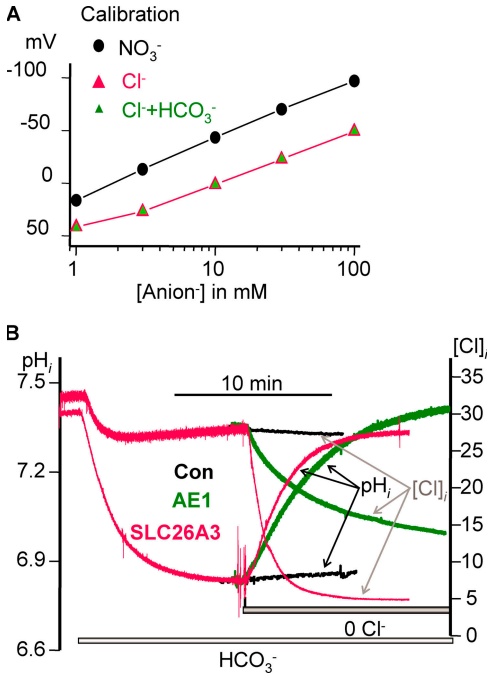

Figure 1. Stoichiometry of Cl^-/HCO_3^- exchange by slc26a3. (A) An example of a calibration of the Cl^- electrode and that the resin is not sensitive to 90 mM HCO_3^- (green triangles) and is more selective for NO_3^- (black circles) than Cl^- (red triangles). In B, control *Xenopus* oocytes (black traces) and an oocyte expressing AE1 (green traces) or slc26a3 (red traces) were bathed in HCO_3^--buffered media, and, after the stabilization of pH_i, they were incubated in Cl^--free media. The initial rates of pH_i and Cl^-_i changes were used to calculate the fluxes and the Cl^-/HCO_3^- stoichiometry that are listed in Table 1. For simplicity, the changes in pH_i and Cl^-_i caused by exposure to CO_2/HCO_3^- are shown only for the oocyte expressing slc26a3. In this and all other experiments, the traces shown are from representative experiments, and the number of experiments and means are given in the text.

RESULTS

To understand the function of the SLC26 transporters in epithelial Cl^- absorption and HCO_3^- secretion, it is essential to know their transport mechanism (channel or coupled transporter) and, in particular, their Cl^-/HCO_3^- transport stoichiometry. The following paragraphs describe our recent efforts toward achieving these goals.

slc26a3 Cl^-/HCO_3^- Transport Stoichiometry Is $2Cl^-/1HCO_3^-$

To determine the precise Cl^-/HCO_3^- transport stoichiometry of the SLC26 transporters, it is necessary to measure the Cl^- and HCO_3^- fluxes, preferably simultaneously and in the same cells. *Xenopus* oocytes are ideal for this task because they can be impaled with two-ion selective microelectrodes and a reference electrode. In a previous study, we described our procedure of measuring pH_i in *Xenopus* oocytes (Shcheynikov et al., 2004). Fig. 1 A shows an example of a calibration curve with a Cl^--selective

TABLE I

Cl^- and HCO_3^- Fluxes and Stoichiometry of Cl^-/HCO_3^- Exchange by AE1, slc26a3, and slc26a6 Transporters

AE1[a,b]			slc26a3[a,b,c]			slc26a6[a,b,d]		
Cl^-	HCO_3^-	Ratio	Cl^-	HCO_3^-	Ratio	Cl^-	HCO_3^-	Ratio
3.8	3.6	1.06	8.4	4.2	2.00	0.9	1.81	0.5
3.1	3.3	0.94	8.3	4.6	1.80	0.75	1.35	0.56
2.9	3.1	0.96	7.5	3.8	1.97	0.75	1.35	0.56
3.0	3.3	0.92	6.5	3.2	2.03	1.05	1.80	0.58
3.1	3.2	0.98	7.1	3.5	2.03	1.20	2.11	0.57
2.3	2.4	0.97	6.2	3.5	1.77	0.75	1.53	0.49
2.5	2.5	1.00	5.2	2.7	1.93	0.90	1.51	0.60
2.8	3.0	0.93	6.7	3.7	1.81	0.60	1.12	0.54
2.9	2.9	0.98	6.6	3.3	1.98	1.00	1.80	0.56
2.9	3.2	0.92	5.9	2.8	2.11	0.75	1.22	0.61
			5.2	2.6	2.00			
			7.6	3.8	2.00			
		0.96 ± 0.04[e]			1.96 ± 0.03[e]			0.56 ± 0.03[e]

[a]All Cl^- and HCO_3^- transport rates are in μM/min recorded upon the first Cl^- removal of oocytes incubated in HCO_3^--buffered media ($Cl^-_{in}/HCO_3^-_{out}$ exchange).

[b]The first sets of Cl^- and HCO_3^- transport and the ratios for each transporter were taken from Fig. 1 B.

[c]The second and third sets for slc26a3 were taken from Fig. 2 (A and C, respectively).

[d]The second set for slc26a6 was taken from Fig. 8 A.

[e]Mean ± SEM.

electrode with the particular Cl^--selective resin used. Plotting the logarithm of the anion concentrations in standard solutions as a function of the electrode potential yielded a linear slope for Cl^- between 3–100 mM that was not affected by the presence of up to 90 mM HCO_3^- and for NO_3^- between 1–100 mM of ~56 mV/decade change in anion concentration. The slope obtained with NO_3^- was shifted to more negative potentials, indicating that the resin prefers NO_3^- over Cl^-. This precludes measurement of Cl^- in the presence of NO_3^- but should be useful for the measurement of Cl^-/NO_3^- exchange.

The simultaneous measurement of Cl^-_i and pH_i in the oocytes is shown in Fig. 1 B. For controls, water-injected oocytes were incubated in HCO_3^--buffered media that reduced pH_i to ~6.85 and had no effect on Cl^-_i, which averaged 26 ± 1 mM ($n = 6$). Exposing these oocytes to Cl^--free medium resulted in very slow rates

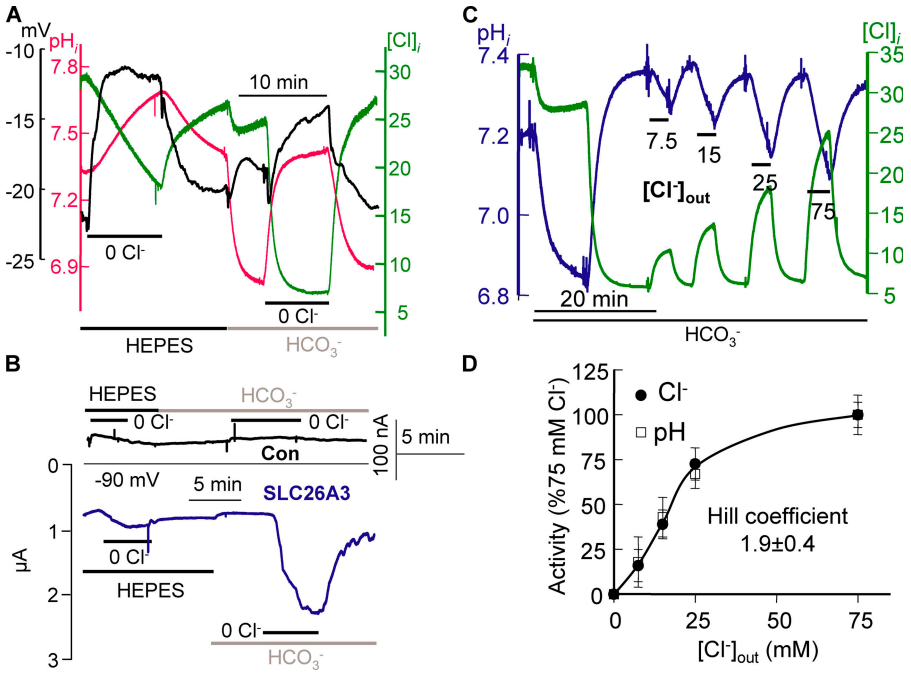

Figure 2. Coupling of Cl^- and HCO_3^- transport by slc26a3. In A, an oocyte expressing slc26a3 was exposed to Cl^--free medium while incubated in HEPES-buffered and HCO_3^--buffered media. Red trace, pH_i; green trace, Cl^-_i; black trace, membrane potential. In B, current generated by Cl^-_i/OH^-_o and $Cl^-_i/HCO_3^-_o$ exchange was measured in a control oocyte (black trace) and an oocyte expressing slc26a3 (blue trace) while holding the membrane potential at −90 mV. In C, an oocyte expressing slc26a3 and incubated in HCO_3^--buffered media was exposed to Cl^--free medium at 10 min and was then exposed to different Cl^-_o between 7.5 and 75 mM, as indicated by the bars, while measuring pH_i (blue trace) or Cl^-_i (green trace). The rates of pH_i (squares) and Cl^-_i (circles) changes from three experiments are summarized in D. Error bars represent SEM.

of increase in pH_i and decrease in Cl^-_i (Fig. 1 B, black traces), which is consistent with the minimal pH_i regulatory capacity of the oocytes reported previously (Boron, 1986). To validate our Cl^- and pH calibration procedures and HCO_3^- and Cl^-_i flux measurements, we expressed the Cl^-/HCO_3^- anion exchanger 1 (AE1) in the oocytes. It is well established that the Cl^-/HCO_3^- transport stoichiometry of this exchanger is 1:1 (Passow, 1986). In this study, when oocytes expressing AE1 and bathed in HCO_3^--buffered media were exposed to Cl^--free media, there was a parallel increase in pH_i and a decrease in Cl^-_i. Calculation of the Cl^-/HCO_3^- flux ratio from the initial rates of the changes in pH_i and Cl^-_i yielded a ratio of 0.96 ± 0.04 (n = 10; Table I). This finding validates our measurement technique, calibration procedures, and determination of the net Cl^- and HCO_3^- fluxes.

The expression of slc26a3 in *Xenopus* oocytes slightly reduced the resting pH_i and set steady-state Cl^- at 29.5 ± 0.9 mM (n = 17), which is statistically different from water-injected oocytes ($P < 0.05$). However, invariably, when the oocytes were exposed to HCO_3^--buffered media, Cl^-_i was reduced to 25.0 ± 0.8 mM (n = 17; $P < 0.01$). Exposing slc26a3-expressing oocytes to Cl^--free medium also increased pH_i and reduced Cl^-_i. However, in the case of slc26a3, the Cl^-/HCO_3^- transport stoichiometry occurred at a ratio of 1.96 ± 0.06 (n = 12; Table I). In all stoichiometry experiments, the slc26a3 and AE1 stoichiometries were measured on the same day and with the same batch of oocytes to further validate the measurements. Hence, the results in Fig. 1 indicate that the slc26a3 Cl^-/HCO_3^- transport stoichiometry is $2Cl^-/1HCO_3^-$.

slc26a3 Functions as a Coupled Exchanger

The $2Cl^-/1HCO_3^-$ stoichiometry of slc26a3 may be the result of tight coupling of the transported ions or may reflect partially uncoupled Cl^- fluxes. The results in Figs. 2 and 3 indicate an initial tight coupling of Cl^- and HCO_3^- transport by slc26a3. It was reported previously that slc26a3 can transport both OH^- and HCO_3^-, although it transports HCO_3^- better than OH^- (Melvin et al., 1999; Ko et al., 2002). This is confirmed in Fig. 2 A, in which we compared Cl^-/OH^- and Cl^-/HCO_3^- exchange by slc26a3. Water-injected oocytes had a resting membrane potential of −39 ± 4 mV (n = 15), and the expression of slc26a3 decreased the membrane potential to −23 ± 4 and −21 ± 4 mV (n = 12) in the absence and presence of HCO_3^-, respectively. Incubation in HEPES- and HCO_3^--buffered Cl^--free media depolarized the membrane potential by 13 ± 3 and 9 ± 3 mV, respectively. Incubating the oocytes in HCO_3^--buffered media similarly increased the rate of pH_i and Cl^-_i changes on exposure to Cl^--free medium.

Attenuation of the change in membrane potential by HCO_3^- was likely caused by the robust Cl^-/HCO_3^- exchange and rapid depletion of Cl^- from the oocytes. This conclusion is supported by comparing the current generated by Cl^-_i/OH^-_o and $Cl^-_i/HCO_3^-_o$ exchange. Because of the $2Cl^-/1HCO_3^-$ stoichiometry, the current was measured at a holding potential of −90 mV. Clamping control oocytes to −90 mV generated an inward current of 0.13 ± 0.04 μA (n = 6). Fig. 2 B shows that in control oocytes, the removal of extracellular Cl^- (Cl^-_o) resulted in a small outward current (black trace). On the other hand, oocytes expressing slc26a3 showed substantial inward current at −90 mV, and the removal of Cl^-_o further increased the inward current (Fig. 2 B, blue trace) as expected from the slc26a3 stoichiometry. Higher current was generated by Cl^-/HCO_3^- compared with Cl^-/OH^- exchange, which is consistent with the higher rate of Cl^-/HCO_3^- exchange in Fig. 2 A. Interestingly, after the initial rapid increase in current on the removal of Cl^-_o, the current continued to increase slowly for several minutes. Development of the slow current parallels the change in pH_i. This may reflect the relief of inhibition of a current-carrying step by the reduction in Cl^-_i or increase in $HCO_3^-_i$ (see models in Fig. 9) or the development of uncoupled HCO_3^- current at continuous incubation in Cl^--free medium that requires the accumulation of HCO_3^- in the oocytes. Uncoupled anion current and channel-like behavior of slc26a3 are illustrated in more detail in the next section. In five experiments, the removal of Cl^-_o in oocytes bathed in HCO_3^--buffered media resulted in a Cl^-/HCO_3^- exchange current of 1.9 ± 0.3 μA. With the Cl^- and HCO_3^- fluxes in Table I, this would suggest that the effective oocyte Cl^- volume is ~285 nl. This relatively low value reflects, in part, the size of the oocytes used and can be influenced by the large surface area of the oocytes. Another potential contributing factor is the development of an uncoupled current with polarity opposite to that generated by slc26a3.

In Fig. 2 (C and D), we measured the Cl^-_o dependency of HCO_3^- and Cl^- transport. To measure the transport at close to the resting pH_i of ~7.4, oocytes bathed in HCO_3^--buffered media were incubated in Cl^--free medium to increase pH_i. After the stabilization of pH_i, the oocytes were alternately exposed to media containing between 7.5 and 75 mM Cl^-_o and to Cl^--free medium. The resulting changes in pH_i and Cl^-_i (Fig. 2 C) were used to determine the rates of the fluxes, which are plotted in Fig. 2 D. It is clear that the slc26a3-mediated Cl^- and HCO_3^- fluxes have the same dependency on Cl^-_o. Interestingly, the Cl^-_o dependence of both anions was similar and had an averaged Hill coefficient of 1.9 ± 0.4 (n = 6 from three experiments), suggesting that $2Cl^-$ ions are transported during each cycle of Cl^-/HCO_3^- exchange, which is consistent with the $2Cl^-/1HCO_3^-$ transport stoichiometry of slc26a3.

Similar acceleration of HCO_3^- and Cl^- transport rates by HCO_3^- and similar dependence of the transport

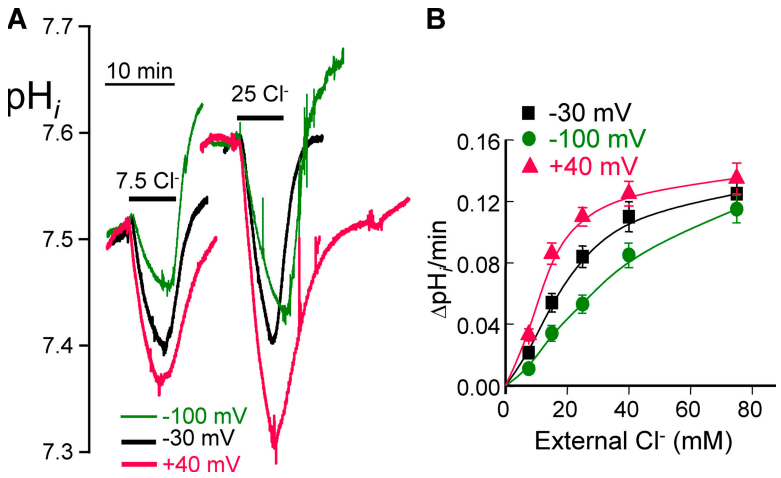

Figure 3. Effect of the membrane potential on HCO_3^- transport by slc26a3. The protocol shown in Fig. 2 C was used to measure changes in pH_i except that the changes in pH_i at each Cl^-_o concentration were measured while holding the membrane potential alternately at −30, −100, and 40 mV. The membrane potential was clamped after the stabilization of Cl^-_i and for 30 s before and during the duration of the subsequent measurement of Cl^-/HCO_3^- exchange. No more that three Cl^- concentrations were tested in each oocyte to minimize error caused by the deterioration of the signal. (A) Example traces from the same oocyte exposed to 7.5 and 25 mM Cl^-_o while holding the membrane potential at −30 (black traces), −100 (green traces), or 40 mV (red traces). Results from at least three measurements at each Cl^- concentration and at the indicated membrane potentials, similar to those in Fig. 3 A, are plotted in B and show the Cl^-_o-dependence of HCO_3^- transport at −30 (squares), −100 (circles), and 40 mV (triangles). Error bars represent SEM.

of the two anions on Cl^-_o suggest tight coupling of Cl^- and HCO_3^- exchange. The $2Cl^-/1HCO_3^-$ transport stoichiometry implies that transport by slc26a3 should be sensitive to the membrane potential. This is illustrated in Fig. 3. In these experiments, oocytes expressing slc26a3 were incubated in HCO_3^--buffered media and then in Cl^--free medium to increase pH_i to physiological levels. Cl^--dependent HCO_3^- efflux and influx were measured by the addition and removal of different concentrations of Cl^-_o, respectively. As expected from the $2Cl^-/1HCO_3^-$ transport stoichiometry of slc26a3, hyperpolarization inhibited Cl^-_o-dependent HCO_3^- efflux and accelerated Cl^-_i-dependent HCO_3^- influx, whereas depolarization had the opposite effects (Fig. 3 A). Measurement of the effect of membrane potential on the Cl^- dependence of Cl^-/HCO_3^- exchange showed that hyperpolarization decreased and depolarization increased the apparent affinity for Cl^-_o (Fig. 3 B). The implication of the effect of the membrane potential for the turnover cycle of Cl^- and HCO_3^- transport by slc26a3 is the stabilization of Cl^-- and HCO_3^--preferring conformations (see Discussion).

Uncoupled Anion Transport by slc26a3

slc26a3 was found to mediate uncoupled anion transport to generate large current, possibly functioning as an anion channel. Evidence for uncoupled transport by slc26a3 was obtained when NO_3^- and SCN^- were used as substrates. Fig. 4 (A and B) shows that replacing Cl^- with NO_3^- in HEPES-buffered media resulted in rapid increase in the outward current measured at +60 mV (NO_3^- influx) but a small increase in the inward current measured at −100 mV. However, the inward current increased with time, reaching a maximum after ~15 min. Immediately after replacing Cl^- with NO_3^-, the reversal potential shifted from −19.8 ± 0.8 to −28.8 ± 1.1 mV ($n = 14$; $P < 0.01$). However, after a 15-min incubation in NO_3^-, the reversal potential returned to that measured in the presence of Cl^-_o, indicating that the increase in inward current is caused by replacing Cl^-_i with $NO_3^-{}_I$ and the permeability of slc26a3 to NO_3^- is higher than that for Cl^-. After a 15- min incubation with NO_3^-, the outward and inward currents increase by 2.68 ± 0.21- and 2.7 ± 0.3-fold ($n = 14$), respectively. Examining the currents with other anions revealed that large currents could be recorded with SCN^- (Fig. 4 C). The current observed with SCN^- was similar to that observed with NO_3^- except that SCN^- increased the current more than NO_3^- (5.8 ± 1.4-fold; $n = 4$).

In a previous study, we were not able to measure appreciable Cl^- current in HEK293 cells expressing slc26a3 (Ko et al., 2004). The increased current measured with NO_3^- (Fig. 4, A and B) offered a new opportunity to determine whether slc26a3 can mediate a current when expressed in HEK293 cells. We used NO_3^- because the cell tolerated NO_3^- better than SCN^-. In Fig. 4 D, the whole cell current was measured in HEK293 cells bathed in HEPES-buffered media and dialyzed with NO_3^-. Incubating control cells in NO_3^- media resulted in a current of 32 ± 7 pA at −100 mV. On the other hand, incubating HEK293 cells expressing slc26a3 in NO_3^--containing media resulted in a current of 238 ± 32 pA at −100 mV, with a reversal potential of

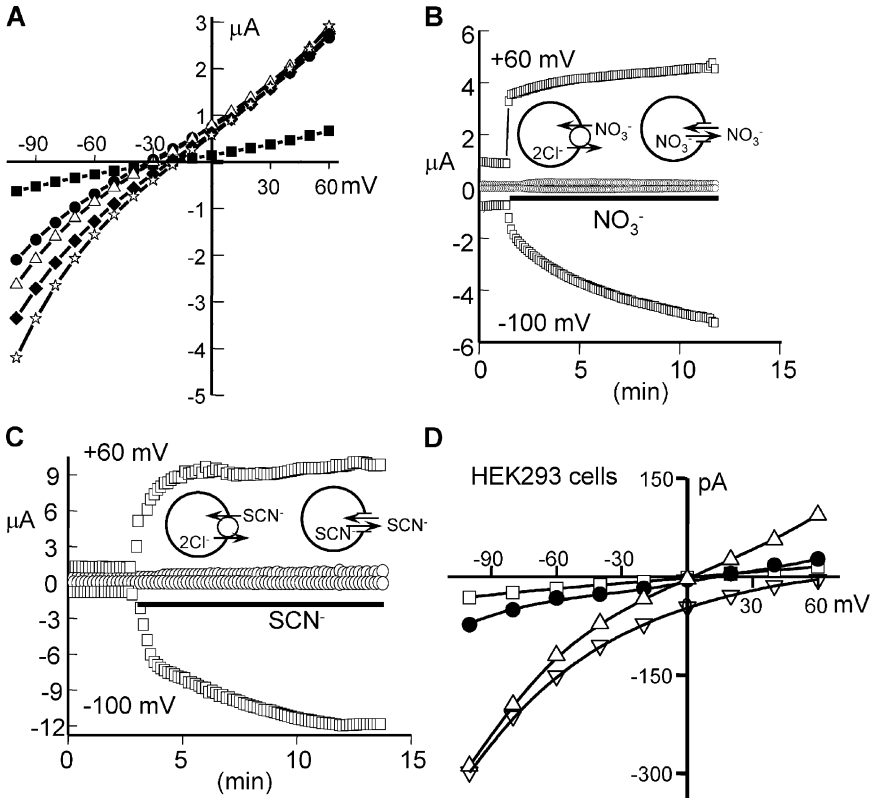

Figure 4. NO_3^- and SCN^- current by slc26a3. *Xenopus* oocytes expressing slc26a3 and bathed in HEPES-buffered media (A–C) were incubated in media in which Cl^-_o was replaced with NO_3^- (A and B) or SCN^- (C) while measuring the I-V relationship (A) or the current (B and C) at a holding membrane potential of −30 mV and sampling every 10 s by stepping to −100 and 60 mV for 50 ms. In A, the oocyte was incubated in Cl^--containing media (squares) or NO_3^--containing media for 1 (circles), 3 (triangles), 5 (diamonds), or 10 min (stars). B and C show the current measured in control (circles) and slc26a3 (squares)-expressing oocytes. The models in B and C show the possible modes of transport at the beginning and end of the incubation period with NO_3^- and SCN^-. (D) The I-V relationship in an HEK293 cell transfected with GFP (squares) or with GFP and slc26a3 and dialyzed with $NO_3^-{}_i$ and incubated in Na^+-free medium in which the major anion was NO_3^- (squares and triangles), gluconate (inverted triangles), or Cl^- (circles). The traces in A–D are from single experiments, and the means and number of experiments are given in the text.

0.3 ± 0.5 mV (n = 10). Replacing extracellular NO_3^- ($NO_3^-{}_o$) with gluconate eliminated the outward current and shifted the reversal potential to 64 ± 2 mV, indicating high selectivity of slc26a3 for NO_3^-. Unexpectedly, in HEK293 cells dialyzed with $NO_3^-{}_i$, replacing $NO_3^-{}_o$ with Cl^-_o markedly reduced both the outward and inward currents. Similarly, when HEK293 cells expressing slc26a3 were dialyzed with Cl^-_i and incubated with $NO_3^-{}_o$, only a small current was measured (unpublished data). The findings in Fig. 4 have several important implications. First, slc26a3 can function as a conductive transporter independent of the expression system. Equally important, the slow development of the inward NO_3^- current in oocytes and the inhibition of the inward NO_3^- current by Cl^-_o in HEK293 cells suggest that Cl^-/NO_3^- exchange is a slow mode of transport that limits the current and that Cl^-_o slows the dissociation of NO_3^- to the external medium to reduce the overall current in HEK293 cells. This also implies that our failure to observe slc26a3-dependent current in HEK293 cells (Ko et al., 2004) was a result of the slow rates of Cl^-/OH^- and Cl^-/HCO_3^- exchange and highlights the usefulness of the oocyte system in this respect.

An increased NO_3^- current could be caused by higher rates of NO_3^-/OH^- and NO_3^-/HCO_3^- exchange than the parallel Cl^- exchange rates or could be caused by uncoupling of the exchange by NO_3^-. To distinguish between these possibilities, we measured the effect of NO_3^- on the membrane potential and pH_i in HEPES- and HCO_3^--buffered media. Fig. 5 (A and B) shows that replacing Cl^-_o with NO_3^- in oocytes incubated in HEPES- or HCO_3^--buffered media resulted in a rapid but transient hyperpolarization by 10.7 ± 0.7 mV (n = 10) and 11.0 ± 1.2 mV (n = 12), respectively. Subsequent replacement of $NO_3^-{}_o$ with Cl^-_o transiently depolarized the cells. The transients are likely caused by the slow accumulation and efflux of NO_3^-, respectively, mediated by Cl^-/NO_3^- exchange. Replacing NO_3^- with gluconate markedly depolarized the cells in both HEPES- and HCO_3^--buffered media (Fig. 5, A and B; last part of the traces). However, in HEPES-buffered media, the depolarization was stable, whereas

in HCO_3^--buffered media, it was transient. The simultaneous measurement of pH_i revealed that the transient change in membrane potential was the result of NO_3^-/HCO_3^- exchange that depleted the oocytes of NO_3^- and returned the membrane potential to the resting level.

Fig. 5 B shows that replacing Cl^-_o with $NO_3^-_o$ further acidified the oocytes by ~0.1 pH units, suggesting that at the acidic pH of 6.85, the NO_3^- gradient is slightly more efficient than the Cl^- gradient in mediating HCO_3^- efflux. However, the addition of NO_3^- to oocytes incubated in Cl^--free medium resulted in marked hyperpolarization but with no reduction in pH_i in HEPES-buffered media and a slow reduction in pH_i in HCO_3^--buffered media (Fig. 5 B, shaded area). Hence, it is clear that slc26a3 can mediate NO_3^-/HCO_3^- exchange. However, $NO_3^-_o/HCO_3^-_i$ exchange occurred at a rate 2.20 ± 0.15-fold (n = 8) slower than $Cl^-_o/HCO_3^-_i$ exchange, whereas the current in the presence of $NO_3^-_o$ was 2.6-fold higher than in the presence of Cl^-_o (Fig. 4). An even more dramatic dissociation between current, membrane potential, and HCO_3^- transport was found with SCN^-. Fig. 5 C shows that the addition of SCN^- to oocytes incubated in Cl^--free

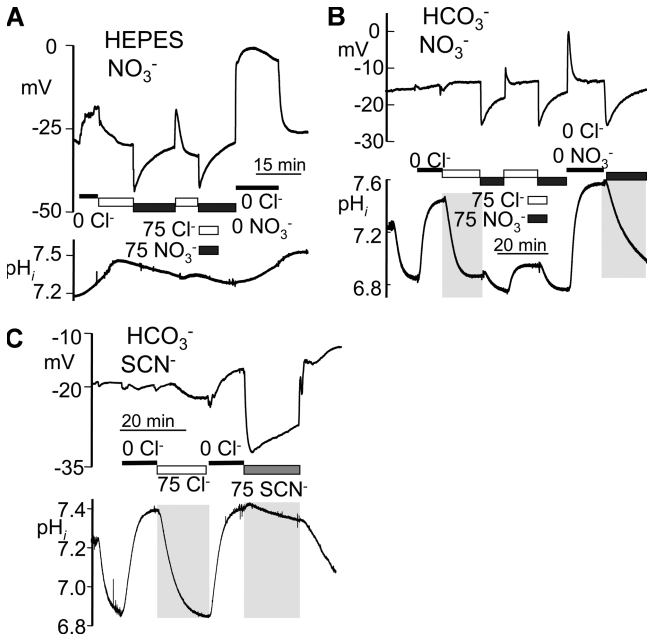

Figure 5. Uncoupled NO_3^- and SCN^- fluxes by slc26a3. *Xenopus* oocytes expressing slc26a3 were bathed in HEPES-buffered (A) or HCO_3^--buffered media (B and C). As indicated by the solid bars, they were exposed to Cl^--free media, and, after the stabilization of pH_i, the rates of Cl^-/HCO_3^- and NO_3^-/HCO_3^- exchange (B) or Cl^-/HCO_3^- and SCN^-/HCO_3^- exchange (C) were compared, as marked by the gray areas. In each panel, the changes in membrane potential are shown in the top trace, and the changes in pH_i are shown in the bottom trace. Note the slow NO_3^-/HCO_3^- exchange and the very slow SCN^-/HCO_3^- exchange. The number of experiments and means are given in the text.

medium stably hyperpolarized the cells by 16.5 ± 0.4 mV (n = 3), but the SCN^-/HCO_3^- exchange occurred at a rate 13.7 ± 1.6-fold slower than that of the Cl^-/HCO_3^- exchange. Uncoupled NO_3^- and SCN^- transport by slc26a3 indicates that slc26a3 has a channel-like activity.

slc26a6 Is an Electrogenic Transporter with a $2HCO_3^-/1Cl^-$ Stoichiometry

Two groups reported that slc26a6 functions as an electrogenic Cl^-/HCO_3^- exchanger (Ko et al., 2002; Xie et al., 2002). In contrast, Chernova et al. (2005) used the SLC26A6 and slc26a6 orthologues to conclude that slc26a6 mediates an electroneutral Cl^-/HCO_3^- exchange. To address this controversy, we measured Cl^-_i, pH_i, and membrane potential in oocytes expressing slc26a6. All of the following experiments were performed with slc26a6 because we and others (Waldegger et al., 2001) found that the SLC26A6 clone is inactive. Fig. 6 A shows that incubating oocytes expressing slc26a6 in HCO_3^--buffered media invariably increased Cl^-_i from 27.1 ± 0.9 to 29.7 ± 1.0 mM ($P < 0.05$; n = 11). This is the opposite from what was found with oocytes expressing slc26a3 (Figs. 1 and 2). Incubating the oocytes in Cl^--free medium in which Cl^- was replaced with gluconate resulted in hyperpolarization of the oocytes from a resting membrane potential of −28 ± 3 to −44 ± 6 mV and −39 ± 5 mV in HEPES- and HCO_3^--buffered media, respectively (n = 10; $P < 0.01$). The hyperpolarization was associated with a significant increase in pH_i but a slow reduction in Cl^-_i. Similar hyperpolarization and changes in pH_i were observed when Cl^- was replaced with $SO_4^=$, indicating that the permeability of slc26a6 to $SO_4^=$ is much lower that that for Cl^- and comparable with that of gluconate. The Cl^-/HCO_3^- flux ratio calculated from the slopes of the pH_i and Cl^-_i changes was found to be 0.56 ± 0.03 (n = 10; Table I), indicating a slc26a6 transport stoichiometry of $2HCO_3^-/1Cl^-$. With a $2HCO_3^-/1Cl^-$ stoichiometry, slc26a6 is expected to generate a current. Because of the relatively slow Cl^-/HCO_3^- exchange by slc26a6 (Table I), the slc26a6-mediated current was resolved at a membrane potential of 40 mV (Fig. 6 B). Incubation of oocytes expressing slc26a6 in HCO_3^--buffered Cl^--free medium and holding the membrane potential at 40 mV resulted in an outward current of 0.76 ± 0.13 μA (n = 4), which is smaller than that mediated by slc26a3, as expected from the slower Cl^-/HCO_3^- exchange by slc26a6.

We have previously reported that slc26a6 expressed in HEK293 cells mediates Cl^-/HCO_3^- and Cl^-/OH^- exchange (Ko et al., 2002). To determine the conductive properties of the exchange, we measured the effect of Cl^- on the current and reversal potential in HEK293 cells expressing slc26a6. Fig. 6 C shows that in symmetrical 150 mM Cl^- and at 60 mV, the expression of

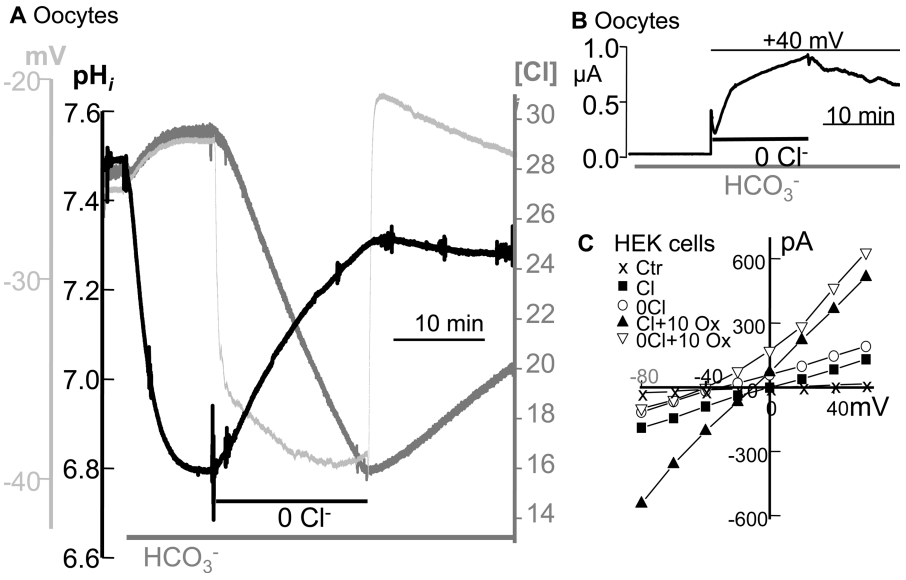

Figure 6. Stoichiometry of Cl^-/HCO_3^- exchange by slc26a6. (A) *Xenopus* oocyte expressing slc26a6 and bathed in HCO_3^--buffered media was incubated in Cl^--free and Cl^--containing medium as indicated. The rates of HCO_3^- (heavy black trace) and Cl^- (heavy gray trace) transport initiated by the removal of Cl^-_o were used to calculate the Cl^-/HCO_3^- transport stoichiometry of slc26a6, and the results of multiple experiments are given in Table 1. The light gray trace shows the change in membrane potential. (B) The current was measured in an oocyte expressing slc26a6 and bathed in HCO_3^--buffered media. Where indicated, the membrane potential was clamped at 40 mV, and the effect of Cl^- removal and readdition on the current was measured. (C) The HEK293 cell expressing slc26a6 was dialyzed with Na^+-free pipette solution containing 150 mM Cl^-_i and bathed in Na^+-free solutions containing 150 mM Cl^- (squares), gluconate (circles), Cl^- and 10 mM oxalate (triangles), or gluconate and oxalate (inverted triangles), and the I-V relationship was determined between −80 and 60 mV. The number of experiments and means are given in the text.

slc26a6 resulted in a current of 196 ± 36 pA ($n = 8$). As was found in oocytes expressing slc26a6 (Ko et al., 2002), the removal of Cl^-_o shifted the reversal potential from 0.5 ± 0.3 to −22 ± 4 mV ($n = 6$). Slc26a6 can also transport formate and oxalate (Ox^{-2}), and Ox^{-2} hyperpolarizes oocytes expressing slc26a6 (Knauf et al., 2001; Jiang et al., 2002). The addition of 10 mM Ox^{-2} to the incubation medium increased the current at 60 mV to 525 ± 48 pA ($n = 8$). In the presence of Cl^-_o, 10 mM Ox^{-2} shifted the reversal potential to −9.2 ± 0.9 mV, and the removal of Cl^-_o resulted in a reversal potential of −43 ± 4 mV ($n = 5$; Fig. 6 B). Hence, slc26a6 also behaves as an electrogenic transporter in HEK293 cells.

Another finding presented in Fig. 6 A is that readdition of Cl^-_o resulted in slow rates of Cl^- influx and HCO_3^- efflux. This can be explained by the rapid depolarization of the membrane potential that disfavors a $2HCO_3^-{}_i/1Cl^-_o$ exchange that moves a negative charge out of the oocytes. This interpretation can be tested by examining whether changes in the membrane potential will have the predicted effect on the fluxes. The results of such tests are shown in Fig. 7 A. The first part of the top traces in Fig. 7 A show that holding the membrane potential at 40 mV accelerated the rate of $HCO_3^-{}_o/Cl^-_i$ exchange and completely halted the $HCO_3^-{}_i/Cl^-_o$ exchange initiated by the readdition of Cl^-_o. On the other hand, holding the membrane potential at −100 mV accelerated $Cl^-_o/HCO_3^-{}_i$ exchange and completely stopped $HCO_3^-{}_o/Cl^-_i$ exchange, which was relieved by switching the membrane potential to 40 mV (Fig. 7 B). These findings are the exact behavior predicted for a $2HCO_3^-/1Cl^-$ exchanger.

slc26a6 Is a Coupled Cl^-/HCO_3^- Exchanger

To determine whether Cl^- and HCO_3^- transport by slc26a6 are coupled, we measured the effect of the membrane potential on Cl^- transport. Fig. 7 C shows that incubating oocytes expressing slc26a6 in a HCO_3^--buffered Cl^--free medium resulted in the typical Cl^- efflux, and the readdition of Cl^-_o resulted in a very slow Cl^- influx. Clamping the membrane potential at −100 mV markedly accelerated the rate of Cl^- influx, which stopped on clamping the membrane potential at 40 mV. Accelerating the influx of the negatively charged Cl^- by holding the membrane potential at −100 mV can occur only by an electrogenic process that tightly couples the transport Cl^- to the transport of another anion with a stoichiometry of at least 2:1.

Additional evidence for the coupling of Cl^- and HCO_3^- transport by slc26a6 is provided in Fig. 8. Fig. 8 A shows that HCO_3^- similarly accelerates the pH_i and Cl^-_i changes initiated by incubating the oocytes in Cl^--free medium. In Fig. 8 (B and C), inhibition by DIDS of Cl^- and HCO_3^- fluxes and membrane hyperpolarization were compared in the same cells. All parameters were similarly inhibited by 1 and 5 μM DIDS. DIDS similarly inhibited the hyperpolarization measured in HEPES-buffered media. The combined results in Figs. 7 and 8 allow us to conclude that slc26a6 functions as a coupled Cl^-/HCO_3^- exchanger.

DISCUSSION

Mutations in several SLC26 transporters are linked to human diseases, most of which involve epithelia dysfunction in specific organs. This indicates that SLC26

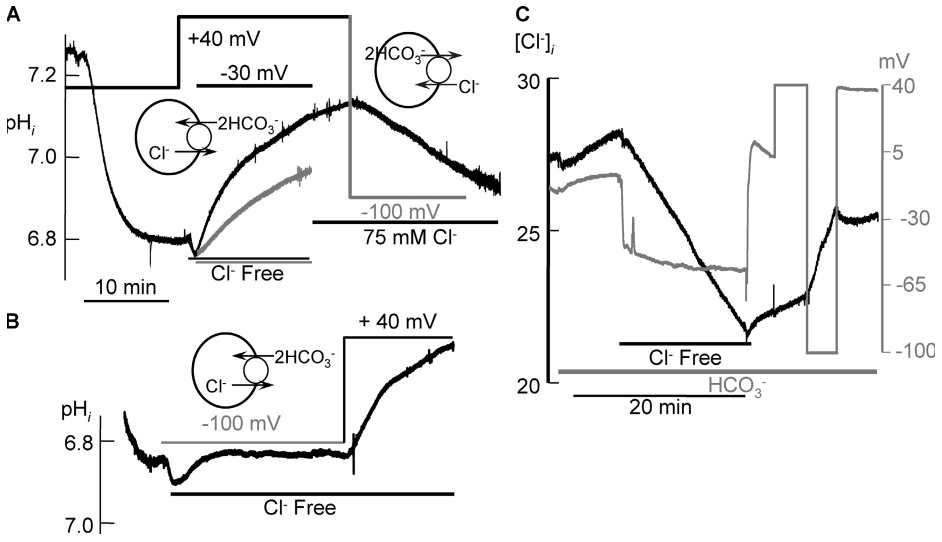

Figure 7. Effect of the membrane potential on HCO_3^- and Cl^- transport by slc26a6. A *Xenopus* oocyte expressing slc26a6 was bathed in HCO_3^--buffered media. (A) After the stabilization of pH_i, the membrane potential was clamped at −30 (gray trace) or 40 mV (black trace) before exposing the oocyte to Cl^--free medium. Where indicated, Cl^-_o was restored, and, after an additional 5 min, the membrane potential was switched from 40 to −100 mV (gray period). (B) After stabilization of the pH_i of the oocyte incubated in HCO_3^--buffered media, the membrane potential was clamped at −100 mV, and the oocyte was exposed to Cl^--free medium (gray period). Where indicated by the black period, the membrane potential was switched to 40 mV. The models depict the mode of exchange measured at each period. (C) After the stabilization of Cl^-_i (black trace), the oocyte was incubated in Cl^--free medium without holding the membrane potential was then incubated in the presence of Cl^-_o while holding the membrane potential at 40 or −100 mV as indicated. Note the initiation of Cl^- influx into the oocytes by holding the membrane potential at −100 mV. Each experiment is representative of at least three others with similar results.

transporters play a central role in transepithelial fluid and electrolyte transport, including Cl^- absorption and HCO_3^- secretion by the kidney, the GI tract, and secretory glands (Kunzelmann and Mall, 2002; Ko et al., 2004; Melvin et al., 2005; Steward et al., 2005). To understand the function of the SLC26 transporters in epithelial Cl^- absorption and HCO_3^- secretion, it is essential to know their transport mechanism and Cl^-/HCO_3^- transport stoichiometry. Two of the most studied SLC26 transporters are slc26a3 and slc26a6. Both were shown to function as Cl^-/HCO_3^- exchangers (Melvin et al., 1999; Ko et al., 2002; Wang et al., 2002) and as electrogenic transporters (Ko et al., 2002; Xie et al., 2002) with isoform-specific stoichiometry (Ko et al., 2002). However, the electrogenicity of the transporters was called into question by a recent study claiming that slc26a6 mediates electroneutral Cl^-/HCO_3^- exchange based on the inability to measure OH^- or HCO_3^--dependent Cl^- current in *Xenopus* oocytes expressing slc26a6 (Chernova et al., 2005). The critical importance of resolving this issue for understanding epithelial Cl^- absorption and HCO_3^- secretion in the normal and disease states requires precise knowledge of the function of these transporters and their stoichiometry.

In this study, we measured all critical parameters, HCO_3^- and Cl^- fluxes, and membrane current and potential in the same cells to determine the Cl^-/HCO_3^- transport stoichiometry and transport mechanism of slc26a3 and slc26a6. The procedure for measuring Cl^-/HCO_3^- exchange stoichiometry was validated by determining a $1Cl^-/1HCO_3^-$ exchange stoichiometry for AE1 (Passow, 1986). With this technique, we proceeded to determine a $2Cl^-/1HCO_3^-$ exchange stoichiometry for slc26a3 and a $1Cl^-/2HCO_3^-$ stoichiometry for slc26a6. Indeed, transport by slc26a3 and slc26a6 was affected by the membrane potential in a manner consistent with their respective stoichiometries. Both transporters appear to function as coupled exchangers. For slc26a3, this conclusion is based on the similar acceleration of HCO_3^- and Cl^- transport by HCO_3^-, similar dependence of the Cl^- and HCO_3^- transport on Cl^-_o (Fig. 2), and stimulation of HCO_3^- influx by clamping the membrane potential at −100 mV (Fig. 3). Tight coupling of Cl^-/HCO_3^- exchange by slc26a6 is supported by the similar acceleration of Cl^- and HCO_3^- transport by HCO_3^-, similar inhibition by DIDS (Fig. 8), and stimulation of Cl^- influx by holding the membrane potential at −100 mV (Fig. 7).

Although the $2Cl^-/1HCO_3^-$ stoichiometry (Table I), a 1.9 Hill coefficient for Cl^- (Fig. 2 D), the stimulation of the negatively charged HCO_3^- influx by holding the membrane potential at −100 mV (Fig. 3 A), the effect of the membrane potential of the Cl^- and HCO_3^- fluxes (Fig. 3 B), and the very large uncoupled NO_3^- and SCN^- currents (Fig. 4) all point to electrogenic transport by slc26a3, two observations need further considerations. The first is the small change in membrane potential observed on the removal of Cl^-_o in slc26a3-expressing oocytes bathed in HCO_3^--buffered media (Figs. 2 A and 5, B and C). We note that completion of the depolarization as a result of the removal of Cl^-_o in HEPES-buffered media required >3 min with the large oocytes (Figs. 2 A and 5 A). At this time, the oocytes lost ∼18 mM of their Cl^-, which can account for the small residual change in membrane potential. The second problematic observation is that the current mediated by

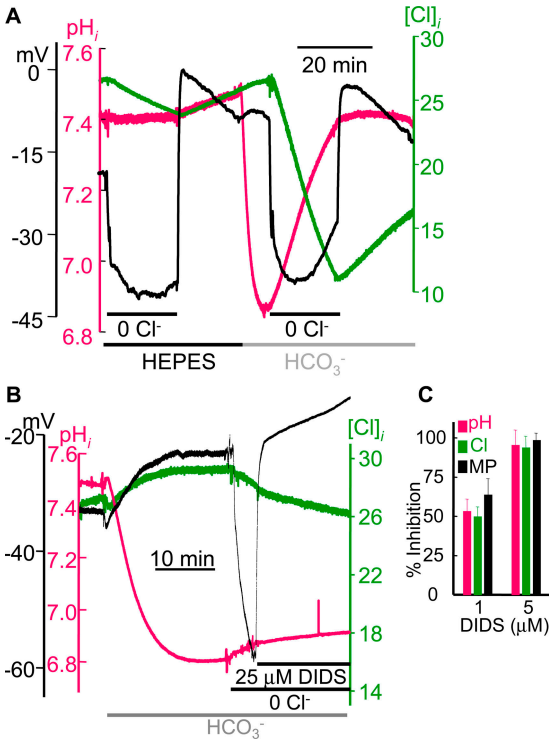

Figure 8. Coupling of Cl^- and HCO_3^- transport by slc26a6. (A) An oocyte expressing slc26a6 was incubated in Cl^--free medium while bathed in HEPES-buffered and HCO_3^--buffered media. Red trace, pH_i; green trace, Cl^-_i; black trace, membrane potential. This experiment is representative of three others with similar results. (B) An oocyte expressing slc26a6 and bathed in HCO_3^--buffered media was incubated in Cl^--free medium, and, shortly after the removal of Cl^-_o, 25 μM DIDS was added to the perfusate, which halted the Cl^- (green trace) and HCO_3^- (red trace) fluxes and reversed the hyperpolarization (black trace). (C) Summary of the changes in pH_i (red bars), Cl^-_i (green bars), and membrane potential (MP; black bars) recorded in four experiments in which oocytes expressing slc26a6 bathed in HCO_3^--buffered media were incubated with either 1 or 5 μM DIDS before the incubation in Cl^--free media that contained the respective concentrations of DIDS. The effect of preincubation with 25 μM DIDS, which completely inhibited the fluxes and the associated change in membrane potential, was taken as 100% to calculate the percent inhibition by 1 and 5 μM DIDS. Error bars represent SEM.

slc26a3 is smaller than that expected from the coupled Cl^- and HCO_3^- fluxes. One possible explanation for this observation is the development of an uncoupled anion current during the incubation in Cl^--free medium that may carry Cl^- and/or HCO_3^-, which will result in an apparent reduced slc26a3-mediated current. Further work is needed to resolve this uncertainty.

The effect of the membrane potential on the apparent affinity for Cl^-_o suggests the turnover cycle for coupled Cl^- and HCO_3^- transport by slc26a3 that is depicted in Fig. 9 A. The model is based on the stabilization of a Cl^-- or HCO_3^--preferring conformation of slc26a3 by the membrane potential. The extracellular-facing substrate-binding sites of the empty transporter (Eo)

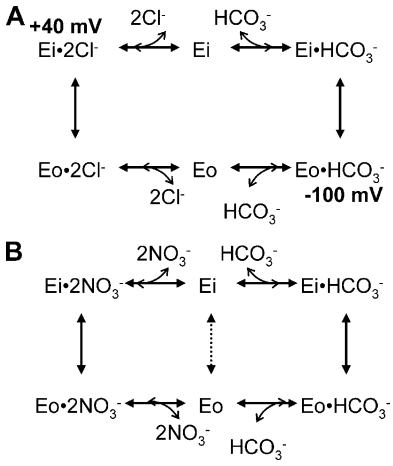

Figure 9. Models of coupled and uncoupled anion transport by slc26a3. (A) A model of the turnover cycle of coupled $2Cl^-/1HCO_3^-$ exchange by slc26a3. (B) A model for the turnover cycles of uncoupled NO_3^- and SCN^- transport by slc26a3.

prefers Cl^- over HCO_3^- and can bind $2Cl^-$ ions to form $Eo•2Cl^-$. $Eo•2Cl^-$ undergoes a conformational change to $Ei•2Cl^-$ and transfers the Cl^- into the cytosol. The cytosolic form of slc26a3 (Ei) prefers HCO_3^- over Cl^- to dissociate the Cl^- and bind HCO_3^- to form $Ei•HCO_3^-$. $Ei•HCO_3^-$ undergoes a conformational transition to $Eo•HCO_3^-$ to transfer and release HCO_3^- to the external medium and complete the cycle. Clamping the membrane potential at 40 mV will favor the Cl^--binding conformation of slc26a3 and shifts the steady-state levels toward the $Ei•2Cl^-$ conformation, resulting in increased apparent affinity for Cl^-. On the other hand, clamping the membrane potential at −100 mV will favor the HCO_3^--binding conformation of slc26a3 to shift the steady-state levels toward the $Eo•HCO_3^-$ conformation, resulting in decreased apparent affinity for Cl^-. Eo and Ei can have the same or different charge. For example, the substrate-binding site of Ei may have two positive charges, binds $1HCO_3^-$ to have a net positive charge, and will be stabilized by a negative membrane potential to reduce the apparent affinity for Cl^-. The substrate-binding site of Eo may have one positive charge, binds $2Cl^-$ to have a net negative charge, and will be stabilized by a positive membrane potential to increase the apparent affinity for Cl^-. The change in the substrate site charge takes place after dissociation of the respective anions. Alternatively, Eo and Ei may have two positive charges, and only the HCO_3^--bound Ei has a net positive charge to be stabilized by negative membrane potential and reduce the apparent affinity for Cl^-. At present, we cannot distinguish between the potential mechanisms.

Interestingly, slc26a3 can mediate a channel-like transport by functioning as an uncoupled anion transporter to mediate large NO_3^- and SCN^- currents that

are not coupled to OH^- or HCO_3^- transport (Figs. 4 and 5). That is, slc26a3 functions as a NO_3^- and SCN^- conductive transporter rather than as an exchanger. slc26a3 can generate NO_3^- and SCN^- currents either by functioning as a NO_3^- and SCN^- channel or as an electrogenic carrier, as depicted in Fig. 9 B for NO_3^-. Functioning as a carrier requires that after the dissociation of NO_3^- or SCN^-, the empty carrier can undergo a conformational change to display the substrate-binding sites facing the cell interior or exterior (Fig. 9 B, dashed arrow) and that in the presence of NO_3^- or SCN^-, the conformational change of the empty carrier is preferential to that of the carrier occupied with HCO_3^-. In contrast, Cl^- disfavors the conformational change of the empty carrier to recouple the transport. This can be because the affinity of the carrier for Cl^- is higher than that for NO_3^- and SCN^- so that only a minute fraction or none of the carrier is empty. The cardinal difference between a channel and uncoupled carrier mode is that a carrier mode requires conformational changes to alternately display the substrate-binding sites to the cell interior and exterior, whereas a channel only requires the transporter to be in an open or closed state. Both modes of transport by the same protein have been described previously. For example, the neurotransmitter transporters can function as coupled carriers or as channels (Kanner and Borre, 2002), whereas a recent study showed that the prokaryotic homologue of the WT ClC Cl^- channels ClC-ec1 functions as an electrogenic H^+-Cl^- exchanger, but its E148A mutant functions exclusively as a Cl^- channel (Accardi and Miller, 2004). This is reminiscent of the Cl^- and NO_3^-/SCN^- transport by slc26a3. A simple way to distinguish between a channel and a carrier mode is to measure single channel activity and observe whether the transporter can switch between discrete open and closed states.

Despite extensive efforts and examination of many experimental conditions, we were unable to measure single channel activity with slc26a3 expressed either in oocytes or in HEK293 cells. Although this would favor an uncoupled carrier mode, negative results must be interpreted with caution. For example, it was suggested that the Cl^-/HCO_3^- exchanger AE1 may mediate a current by occasionally letting the ions move along a channel-like pathway in an uncoupled slippage-like manner (Frohlich, 1984). This may generate a small current that is difficult to detect by single channel measurement. NO_3^- and SCN^- transport by slc26a3 may be mediated, in part, by such a mechanism. Therefore, at present, our results are not sufficient to state with confidence which model more accurately describes the NO_3^- and SCN^- currents by slc26a3. Nevertheless, it is clear that slc26a3 can function as a coupled $2Cl^-/1HCO_3^-$ exchanger or as an uncoupled transporter to mediate anion currents. However, in the presence of physiological Cl^- and HCO_3^- gradients, the preferential mode of transport by slc26a3 is a coupled $2Cl^-/1HCO_3^-$ exchange.

The current findings concerning the properties of slc26a6 are in agreement with two previous studies (Ko et al., 2002; Xie et al., 2002) but contradict another (Chernova et al., 2005) concluding that slc26a6 is an electroneutral Cl^-/HCO_3^- exchanger. However, Chernova et al. (2005) did not measure the stoichiometry of the transport, and their findings have internal inconsistencies. For example, they reported that hSLC26A6 and mslc26a6 mediate the same Cl^-/HCO_3^- exchange activity, yet mslc26a6 showed close to 100-fold higher Cl^- fluxes than hSLC26A6 (Chernova et al., 2005). This calls into question their measurement of pH_i with BCECF in the large oocytes and whether these measurements reflect net HCO_3^- transport by slc26a6. In addition, Chernova et al. (2005) reported similar Ox^{-2} transport by hSLC26A6 and mslc26a6 but also that Ox^{-2} affected the membrane potential of oocytes expressing mslc26a6 but not hSLC26A6. The size of the current in the oocytes expressing hSLC26A6 and mslc26a6 in the presence and absence of Ox^{-2} was small with poor signal/noise (Chernova et al., 2005). As shown in Fig. 6, Ox^{-2} must cause a large increase in the current, and the increase should be independent of the slc26a6 isoform used for the current measurements to be valid.

The Cl^-/HCO_3^- transport stoichiometry of slc26a3 and slc26a6 has profound significance for the mechanism of epithelial Cl^- absorption and HCO_3^- secretion. Thus, as discussed in a previous study (Ko et al., 2004) and reviewed in Steward et al. (2005), the axial distribution of these transporters in secretory epithelia, their interaction with CFTR, and regulation of their function (Ko et al., 2002, 2004) determines the final Cl^- and HCO_3^- concentrations of the secreted fluid. The stoichiometry of slc26a3 and slc26a6 is suitable for absorbing the Cl^- and concentrating HCO_3^- in the secreted fluid. At luminal membrane potentials more depolarized than -50 mV, slc26a6 in the proximal duct and slc26a3 in the distal duct will determine the final Cl^- and HCO_3^- concentrations of HCO_3^--rich and Cl^--poor fluids such as those secreted by the pancreas and salivary glands (Ko et al., 2004). However, at more hyperpolarized voltages and at Cl^-_i that is at or <4 mM, the opposite arrangement is more favorable (Steward et al., 2005). The Cl^- and HCO_3^- content of fluids generated by epithelia are of vital importance for the integrity and function of these organs, as evident from their destruction in cystic fibrosis, a disease typified by aberrant Cl^- absorption and HCO_3^- secretion (Wilschanski and Durie, 1998; Sokol, 2001).

This work was supported by National Institutes of Health grants DE12309 and DK38938 and the Cystic Fibrosis Foundation grant MUALLE01G0.

Olaf S. Andersen served as editor.

Submitted: 23 August 2005
Accepted: 17 March 2006

REFERENCES

Accardi, A., and C. Miller. 2004. Secondary active transport mediated by a prokaryotic homologue of ClC Cl- channels. *Nature.* 427:803–807.

Bissig, M., B. Hagenbuch, B. Stieger, T. Koller, and P.J. Meier. 1994. Functional expression cloning of the canalicular sulfate transport system of rat hepatocytes. *J. Biol. Chem.* 269:3017–3021.

Boron, W.F. 1986. Intracellular pH regulation in epithelial cells. *Annu. Rev. Physiol.* 48:377–388.

Chernova, M.N., L. Jiang, D.J. Friedman, R.B. Darman, H. Lohi, J. Kere, D.H. Vandorpe, and S.L. Alper. 2005. Functional comparison of mouse slc26a6 anion exchanger with human SLC26A6 polypeptide variants: differences in anion selectivity, regulation, and electrogenicity. *J. Biol. Chem.* 280:8564–8580.

Cook, D.I., E.W. Van Lennep, M.L. Roberts, and J.A. Young. 1994. Secretion by the major salivary glands. *In* Textbook of Physiology of the Gastrointestinal Tract. L.R. Johnson, editor. Raven Press, New York. 1061–1117.

Dudas, P.L., S. Mentone, C.F. Greineder, D. Biemesderfer, and P.S. Aronson. 2006. Immunolocalization of anion transporter Slc26a7 in mouse kidney. *Am. J. Physiol. Renal Physiol.* 290: F937–F945.

Everett, L.A., B. Glaser, J.C. Beck, J.R. Idol, A. Buchs, M. Heyman, F. Adawi, E. Hazani, E. Nassir, A.D. Baxevanis, et al. 1997. Pendred syndrome is caused by mutation in a putative sulphate transporter gene (PDS). *Nat. Genet.* 17:411–422.

Forlino, A., R. Piazza, C. Tiveron, S. Della Torre, L. Tatangelo, L. Bonafe, B. Gualeni, A. Romano, F. Pecora, A. Superti-Furga, et al. 2005. A diastrophic dysplasia sulfate transporter (SLC26A2) mutant mouse: morphological and biochemical characterization of the resulting chondrodysplasia phenotype. *Hum. Mol. Genet.* 14:859–871.

Frohlich, O. 1984. Relative contributions of the slippage and tunneling mechanisms to anion net efflux from human erythrocytes. *J. Gen. Physiol.* 84:877–893.

Frohlich, O. 1988. The "tunneling" mode of biological carrier-mediated transport. *J. Membr. Biol.* 101:189–198.

Hamer, W.J., and Y.-C. Wu. 1972. Osmotic coefficient and mean activity coefficients of uni-univalent electrolytes in water at 25°C. *J. Phys. Chem. Ref. Data.* 1:1047–1099.

Hästbacka, J., A. de la Chapelle, M.M. Mahtani, G. Clines, M.P. Reeve-Daly, M. Daly, B.A. Hamilton, K. Kusumi, B. Trivedi, and A. Weaver, et al. 1994. The diastrophic dysplasia gene encodes a novel sulfate transporter: positional cloning by fine-structure linkage disequilibrium mapping. *Cell.* 78:1073–1087.

Ianowski, J.P., R.J. Christensen, and M.J. O'Donnell. 2002. Intracellular ion activities in Malpighian tubule cells of *Rhodnius prolixus*: evaluation of Na+-K+-2Cl- cotransport across the basolateral membrane. *J. Exp. Biol.* 205:1645–1655.

Irokawa, T., M.E. Krouse, N.S. Joo, J.V. Wu, and J.J. Wine. 2004. A "virtual gland" method for quantifying epithelial fluid secretion. *Am. J. Physiol. Lung Cell. Mol. Physiol.* 287:L784–L793.

Jiang, Z., I.I. Grichtchenko, W.F. Boron, and P.S. Aronson. 2002. Specificity of anion exchange mediated by mouse SLc26a6. *J. Biol. Chem.* 277:33963–33967.

Kanner, B.I., and L. Borre. 2002. The dual-function glutamate transporters: structure and molecular characterisation of the substrate-binding sites. *Biochim. Biophys. Acta.* 1555:92–95.

Kim, K.H., N. Shcheynikov, Y. Wang, and S. Muallem. 2005. SLC26A7 is a Cl^- channel regulated by intracellular pH. *J. Biol. Chem.* 280:6463–6470.

Knauf, F., C.L. Yang, R.B. Thomson, S.A. Mentone, G. Giebisch, and P.S. Aronson. 2001. Identification of a chloride-formate exchanger expressed on the brush border membrane of renal proximal tubule cells. *Proc. Natl. Acad. Sci. USA.* 98:9425–9430.

Ko, S.B., N. Shcheynikov, J.Y. Choi, X. Luo, K. Ishibashi, P.J. Thomas, J.Y. Kim, K.H. Kim, M.G. Lee, S. Naruse, and S. Muallem. 2002. A molecular mechanism for aberrant CFTR-dependent HCO_3^- transport in cystic fibrosis. *EMBO J.* 21:5662–5672.

Ko, S.B., W. Zeng, M.R. Dorwart, X. Luo, K.H. Kim, L. Millen, H. Goto, S. Naruse, A. Soyombo, P.J. Thomas, and S. Muallem. 2004. Gating of CFTR by STAS domain of SLC26 transporters. *Nat. Cell Biol.* 6:343–350.

Kunzelmann, K., and M. Mall. 2002. Electrolyte transport in the mammalian colon: mechanisms and implications for disease. *Physiol. Rev.* 82:245–289.

Liu, X.Z., X.M. Ouyang, X.J. Xia, J. Zheng, A. Pandya, F. Li, L.L. Du, K.O. Welch, C. Petit, R.J. Smith, et al. 2003. Prestin, a cochlear motor protein, is defective in non-syndromic hearing loss. *Hum. Mol. Genet.* 12:1155–1162.

Makela, S., J. Kere, C. Holmberg, and P. Hoglund. 2002. SLC26A3 mutations in congenital chloride diarrhea. *Hum. Mutat.* 20:425–438.

Melvin, J.E., K. Park, L. Richardson, P.J. Schultheis, and G.E. Shull. 1999. Mouse down-regulated in adenoma (DRA) is an intestinal Cl^-/HCO_3^- exchanger and is up-regulated in colon of mice lacking the NHE3 Na^+/H^+ exchanger. *J. Biol. Chem.* 274:22855–22861.

Melvin, J.E., D. Yule, T. Shuttleworth, and T. Begenisich. 2005. Regulation of fluid and electrolyte secretion in salivary gland acinar cells. *Annu. Rev. Physiol.* 67:445–469.

Mount, D.B., and M.F. Romero. 2004. The SLC26 gene family of multifunctional anion exchangers. *Pflugers. Arch.* 447:710–721.

Nakada, T., K. Zandi-Nejad, Y. Kurita, H. Kudo, V. Broumand, C.Y. Kwon, A. Mercado, D.B. Mount, and S. Hirose. 2005. Roles of Slc13a1 and Slc26a1 sulfate transporters of eel kidney in sulfate homeostasis and osmoregulation in freshwater. *Am. J. Physiol. Regul. Integr. Comp. Physiol.* 289:R575–R585.

Passow, H. 1986. Molecular aspects of band 3 protein-mediated anion transport across the red blood cell membrane. *Rev. Physiol. Biochem. Pharmacol.* 103:62–203.

Petrovic, S., S. Barone, J. Xu, L. Conforti, L. Ma, M. Kujala, J. Kere, and M. Soleimani. 2004. SLC26A7: a basolateral Cl-/HCO3-exchanger specific to intercalated cells of the outer medullary collecting duct. *Am. J. Physiol. Renal Physiol.* 286:F161–F169.

Regeer, R.R., A. Lee, and D. Markovich. 2003. Characterization of the human sulfate anion transporter (hsat-1) protein and gene (SAT1; SLC26A1). *DNA Cell Biol.* 22:107–117.

Roos, A., and W.F. Boron. 1981. Intracellular pH. *Physiol. Rev.* 61:296–434.

Royaux, I.E., S.M. Wall, L.P. Karniski, L.A. Everett, K. Suzuki, M.A. Knepper, and E.D. Green. 2001. Pendrin, encoded by the Pendred syndrome gene, resides in the apical region of renal intercalated cells and mediates bicarbonate secretion. *Proc. Natl. Acad. Sci. USA.* 98:4221–4226.

Shcheynikov, N., K.H. Kim, K.M. Kim, M.R. Dorwart, S.B. Ko, H. Goto, S. Naruse, P.J. Thomas, and S. Muallem. 2004. Dynamic control of cystic fibrosis transmembrane conductance regulator Cl(-)/HCO3(-) selectivity by external Cl(-). *J. Biol. Chem.* 279:21857–21865.

Sokol, R.Z. 2001. Infertility in men with cystic fibrosis. *Curr. Opin. Pulm. Med.* 7:421–426.

Soleimani, M., T. Greeley, S. Petrovic, Z. Wang, H. Amlal, P. Kopp, and C.E. Burnham. 2001. Pendrin: an apical Cl-/OH-/HCO3-exchanger in the kidney cortex. *Am. J. Physiol. Renal Physiol.* 280:F356–F364.

Steward, M.C., H. Ishiguro, and R.M. Case. 2005. Mechanisms of bicarbonate secretion in the pancreatic duct. *Annu. Rev. Physiol.* 67:377–409.

Superti-Furga, A., J. Hastbacka, W.R. Wilcox, D.H. Cohn, H.J. van der Harten, A. Rossi, N. Blau, D.L. Rimoin, B. Steinmann, E.S. Lander, and R. Gitzelmann. 1996. Achondrogenesis type IB is caused by mutations in the diastrophic dysplasia sulphate transporter gene. *Nat. Genet.* 12:100–102.

Verlander, J.W., K.A. Hassell, I.E. Royaux, D.M. Glapion, M.E. Wang, L.A. Everett, E.D. Green, and S.M. Wall. 2003. Deoxycorticosterone upregulates PDS (Slc26a4) in mouse kidney: role of pendrin in mineralocorticoid-induced hypertension. *Hypertension.* 42:356–362.

Xie, Q., R. Welch, A. Mercado, M.F. Romero, and D.B. Mount. 2002. Molecular characterization of the murine SLc26a6 anion exchanger: functional comparison with SLc26a1. *Am. J. Physiol. Renal Physiol.* 283:F826–F838.

Xu, J., J. Henriksnas, S. Barone, D. Witte, G.E. Shull, J.G. Forte, L. Holm, and M. Soleimani. 2005. SLC26A9 is expressed in gastric surface epithelial cells, mediates Cl^-/HCO_3^- exchange, and is inhibited by NH_4^+. *Am. J. Physiol. Cell Physiol.* 289:C493–C505.

Waldegger, S., I. Moschen, A. Ramirez, R.J. Smith, H. Ayadi, F. Lang, and C. Kubisch. 2001. Cloning and characterization of SLC26A6, a novel member of the solute carrier 26 gene family. *Genomics.* 72:43–50.

Wang, Z., S. Petrovic, E. Mann, and M. Soleimani. 2002. Identification of the apical Cl^-/HCO_3^- exchanger in the small intestine. *Am. J. Physiol. Gastrointest. Liver Physiol.* 282:G573–G579.

Wang, Z., T. Wang, S. Petrovic, B. Tuo, B. Riederer, S. Barone, J.N. Lorenz, U. Seidler, P.S. Aronson, and M. Soleimani. 2005. Renal and intestinal transport defects in SLc26a6-null mice. *Am. J. Physiol. Cell Physiol.* 288:C957–C965.

Wilschanski, M., and P.R. Durie. 1998. Pathology of pancreatic and intestinal disorders in cystic fibrosis. *J. R. Soc. Med.* 91:40–49.